10th South African Conference on Computational and Applied Mechanics
Potchefstroom
3 – 5 October 2016

Heat Transfer in Two and Three-dimensional Single Span Greenhouses

S Kruger[1], L Pretorius[2]

[1]University of Johannesburg
Faculty of Engineering and the Built Environment
Department of Mechanical Engineering Science
Johannesburg, South Africa
skruger@uj.ac.za

[2]University of Pretoria
Faculty of Engineering, the Built Environment and Information Technology, Graduate School of Technology Management
Pretoria, South Africa
Leon.Pretorius@up.ac.za

Email of Corresponding Author: skruger@uj.ac.za

ABSTRACT

The purpose of this paper is to investigate the heat transfer in two-dimensional and three-dimensional cavities representing a single span greenhouse. This investigation is conducted numerically using Computational Fluid Dynamics (CFD). The heat transfer and temperature fields driven by buoyancy forces are investigated. The research commences with the validation of a few fundamental geometries used as the building blocks for a large commercial greenhouse. The first fundamental geometry is a square filled with air. The CFD results for a square cavity are first evaluated against experimental results found in the literature for both two and three dimensional cavities. The heat transfer inside the cavities is then investigated and compared to those found in the literature. A reasonably good comparison between the numerical CFD results and the experimental results was found for both the two- and three-dimensional cavities. Based on the validated CFD models, two three-dimensional single span greenhouses containing a pitched roof were investigated to determine the effect of design alterations on the heat transfer within the cavity. The results were also compared to two-dimensional greenhouses with a 30 and 45 degree roof angle respectively. Results found that there are significant differences between the two and three-dimensional cases when the average Nusselt number is considered, especially for a greenhouse containing a roof angle of 45 degrees. Temperature distributions were also found to vary significantly throughout the three-dimensional greenhouses.

KEYWORDS

Greenhouse, Natural ventilation, Computational Fluid Dynamics

INTRODUCTION

Natural convection has received considerable attention due to its practical interest in a large number of engineering applications. A few examples are the natural or forced convection of buildings, and electronic device cooling. Baines and Turner [1] initially considered this problem by investigating the effect of a small buoyancy source on the environment in a closed space. During mid-season and sunny winters greenhouses are usually fully closed, with buoyancy effects due to warm soil and transpiring leaves the only driving forces present. This situation corresponds to the classic Rayleigh-Bénard convection where a cavity is heated from below and cooled from above. The thermal situation in a closed greenhouse containing a continuous crop canopy surface can be approximated by natural convection in a dry, floor heated cavity [2]. Numerous studies have been performed on three-dimensional cavities. In a study by Leong et al [3] the authors attempted a physically-realizable experiment in a laboratory to be used for CFD validation. The work was extended by Mamun et al [4] to include a new orientation. A cubical air-filled cavity with one pair of opposing faces at different temperatures, the remaining faces with a linear variation from the hot wall to the cold wall was considered. The cavity was tilted at various angles and Nusselt numbers were measured and found to be within an average deviation of 0.3% when compared to the simulation results with the CFD code used. A thorough study consisting of both experimental and numerical work was performed by Baïri [5]. A square cavity at various inclination angles and Rayleigh numbers was investigated. Results were found to agree reasonably well with results published in the literature. For all values of the Rayleigh number investigated, it

was found that the inclination of the cavity played a major role in the convective exchanges. Various turbulence models in unsteady natural convection were assessed by Altaç and Uğurlubilek [6]. Their study revealed that 3D laminar and RANS models resulted in almost similar mean Nusselt number predictions up to Ra = 10^{10}. They also found these predictions to be compatible with results from 2D simulations, but is not the case for larger Rayleigh numbers. Overall their study indicated that 3D RANS models yield more accurate mean Nusselt numbers. In the present work, two and three-dimensional cavities representing a greenhouse with a zero degree roof angle are firstly evaluated against experimental data. The 2D and 3D models are then modified to investigate the effect of design alterations such as roof angle.

COMPUTATIONAL FLUID DYNAMICS

Numerical simulations using Computational Fluid Dynamics (CFD) have been employed quite frequently to investigate natural convection. But experimental work pertaining to natural convection is generally complicated and time consuming. With advances in computer technology, Computational Fluid Dynamics (CFD) has become a valuable research and design tool for the investigation of natural convection. Quantitative predictions of for example fluid flow are based on the laws of conservation (mass, momentum and energy).

In Computational Fluid Dynamics a numerical solution of partial differential equations, typically the Navier-Stokes Equations, is obtained [7]. The transport of mass, momentum and energy in moving fluids are governed by these equations. The transport of the mentioned quantities is governed by three laws: conservation of mass, Newton's second law of motion and the first law of thermodynamics [8].

If a general variable ϕ is introduced, the conservative form of all fluid flow equations can usually be written as shown in Equation (1) [9]:

$$\frac{d(\rho\phi)}{dt} + \mathrm{div}(\rho\phi\bar{u}) = \mathrm{div}(\Gamma \mathrm{grad}\,\phi) + S_\phi \tag{1}$$

Equation 1 is called the transport equation for property φ. This equation emphasizes the various transport processes: the first term on the left-hand side is the rate of change term, while the second term is the convective term. The first term on the right-hand side is the diffusive term (Γ= diffusion coefficient) and the last term is the source term.

In the approach followed in this study the finite volume discretization is the first step in solving these transport equations. This method subdivides the solution domain into a finite number of small control volumes, which corresponds to the cells of a computational grid. Discrete versions of the integral form of the continuum transport equations are applied to each volume. The objective of this method is to obtain a set of algebraic equations. An algebraic multi-grid solver such as the one described in [10] can then be used to solve the resulting equations. The integration of equation 1 over a three-dimensional control volume (CV) is a crucial step in the finite volume method:

$$\frac{d}{dt}\int_{CV}\rho\phi dV + \int_{A}\mathrm{div}(\rho\phi\bar{u})dV = \int_{CV}(\Gamma \mathrm{div}\,\phi)dV + \int_{CV} S_\phi dV \tag{2}$$

The first term on the left hand side indicates the rate of change of the total amount of fluid property φ in the control volume. The product in the second term expresses the flux component of the property φ due to fluid flow along the outward vector n, therefore the second term on the left hand side is the convective term, i.e. the net rate of decrease of fluid property φ of the fluid element due to convection. The first term on the right is the diffusive term and associated with a flux into the element. This term represents the net rate of increase of fluid property φ of the fluid element due to diffusion. The last term represents the rate of increase of property φ due to sources inside the fluid element [9]. A detailed description of a typical discretization procedure can be found in for example Patankar [11].

Two-dimensional Numerical Model – Square Greenhouse

The initial square cavity representing a single-span greenhouse with a zero-degree roof angle presented in this research paper was based on the cavity studied experimentally and numerically by Baïri [5]. The cavity has dimensions of 0.75m x 0.75m. The bottom and top walls were specified as isothermal (heated and cooled

respectively), generating the buoyant flow in the cavity, while the vertical walls were adiabatic. The top wall was assigned a temperature of T_c=15°C, and the temperature on the bottom wall, T_H, was adjusted to achieve different values of the Rayleigh number (Ra). The flow field was assumed to be steady, and the fluid (air) incompressible. The commercial CFD code StarCCM+ [10] was used to perform the numerical analysis. The Rayleigh number was calculated using $\Delta T = T_h - T_c$ associated with the distance L between the two active walls and the following equation:

$$Ra = \frac{g\beta L^3 \Delta T}{\nu \alpha} \tag{3}$$

The properties of air used in the model were calculated using the average temperature between the hot and cold wall (T_{ave}) for each case.

Mesh

The square cavity was meshed for CFD purposes using the polyhedral meshing model included in the StarCCM+ software. As turbulent flow in a square cavity with natural convection is characterized by a thin boundary layer containing relatively large flow gradients, a large number of cells are required in this region. The advancing prism layer meshing model [10] was used to generate these cells in order to adequately capture boundary layer, turbulence effects and heat transfer near the wall boundaries. Four different base sizes were tested to determine mesh independence. The maximum simulated x- and y-velocity components in the CFD domain were monitored, and the average Nusselt number on the hot wall was calculated for each base size. Taking simulation time and available resources into account, it was decided to use a base of 0.016m for all the simulations in this section. The difference between the values is less than 1%, therefore it can be concluded that the results are independent of the cell size. The following models were used in the CFD software to model the physics for the fluid in the square: Ideal Gas, K-Epsilon Turbulence, Low y+ Wall Treatment, Reynolds-Averaged Navier-Stokes, Segregated Flow - Segregated Fluid Temperature, Standard K-Epsilon Low-Re, Steady, Two Dimensional, Gravity. The solution update for the segregated flow model is controlled according to the SIMPLE algorithm [9]. The segregated fluid temperature model was chosen as a companion to the segregated flow model. This model solves the total energy equation with temperature as the solved variable. The equation of state is then used to calculate enthalpy. The model is appropriate for simulations that do not involve combustion [10]. Since only the flow in the turbulent regime will be investigated, the k-epsilon turbulence model was activated. Accurately predicting turbulent buoyant flows are difficult to achieve, and have been successful in only a few cases as illustrated in [12]. This is due to the complexity of the numerical simulation of boundary layers adjacent to the walls, as well as the uncertainty of the general turbulence models for turbulent natural convection [12]. Two turbulence models were tested for the initial case considered here, namely the RANS k-epsilon realizable two-layer model, and the k-epsilon Standard low-Reynolds Number turbulence model. In a study by Henkes et al [13] it was mentioned that various low-Reynolds number models predicted wall heat transfer the closest to the experimental values. The Low-Reynolds number has additional damping functions which allow it to be applied to the viscous boundary layer adjacent to the walls, and is recommended for use in natural convection problems. The low Y+ wall treatment was used in conjunction with the low-Reynolds number turbulence model. It is assumed by this wall treatment that the viscous sublayer is resolved, and wall laws are unnecessary. This wall treatment can however be used only with a fine enough mesh. An initial simulation was done to determine whether the near wall spacing is appropriate for the simulation, i.e. whether the amount of prism layers created on the walls was sufficient. Ten prism layers were initially specified in the mesh setup, with a thickness of 0.01m. The dimensionless Wall Y+ was defined as follows [10]:

$$y^+ = \frac{yu^*}{\nu} \tag{4}$$

Where y is the normal distance from the wall to the wall cell-centroid, u^* is a reference velocity and ν the kinematic viscosity. The dimensionless Wall Y+ values were plotted as a scalar on the wall boundaries of the cavity. They were found to be overall less than 1 for the chosen mesh base size, which implies that the prism layer thickness and amount of prism layer cells are adequate for the chosen turbulence model.

RESULTS – SQUARE GREENHOUSE

Validation – Two-dimensional Square Greenhouse

The CFD simulation results have been published previously [14] and is repeated here for clarity. In order to assess the convective contribution of the heat exchange within the cavity, the surface average Nusselt number (ratio of convective to conductive heat transfer across a boundary) was calculated for the floor of the cavity. The Nusselt number is given by equation 5:

$$Nu = \frac{hL}{k} \tag{5}$$

The surface averaged Nusselt number on the hot floor across all the cells was calculated from the CFD results and compared to results found in the literature as shown in Figure 4.6. A custom user function was written in StarCCM+ which calculated the Nusselt Number for each cell on the hot wall using the boundary heat flux. The syntax can be seen in equation 6:

$$(abs(\$BoundaryHeatFlux)/\Delta T)* L/k \tag{6}$$

The equation essentially takes the absolute value of the boundary heat flux ($ implies it is a scalar function in StarCCM+), divides it by the temperature difference, multiplies the answer by the height of the cavity and lastly divides by the thermal conductivity of the air. The surface averaged Nusselt number was calculated as follows using the scalar-based report function in the software, where the surface averaged Nusselt number was calculated for the hot wall (cavity floor) as shown in equation 7:

$$\text{Surface Averaged Nusselt Number} = \frac{1}{a}\int Nu\, da = \frac{\sum_f Nu_f A_f}{\sum_f A_f} \tag{7}$$

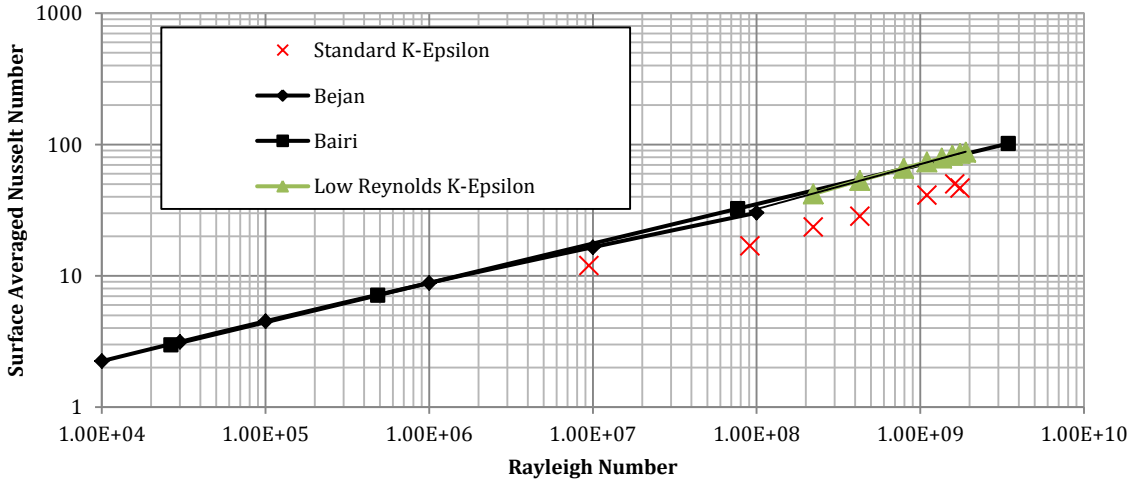

Figure 1: Average Nusselt number along the hot wall vs Rayleigh number

The graph in Figure 1 shows the numerical results for the Nusselt number when applying both the standard realizable k-epsilon turbulence model as well as the LRN k-epsilon turbulence model. Simulations applying the standard realizable k-epsilon turbulence model indicate a relatively large discrepancy when compared to experimental results, as well as the numerical results using the standard low-Reynolds number k-epsilon turbulence model. The results obtained for the low-Reynolds number k-epsilon are essentially in agreement with results published by Baïri [5]. The Nusselt-Rayleigh relationship that best fit the curve was found to be:

$$Nu = 0.0589 Ra^{0.3422} \tag{8}$$

Overall, a relatively good agreement was found between the numerical and experimental results when using the low-Reynolds number k-epsilon turbulence model.

RESULTS – SQUARE GREENHOUSE

Validation - Three-Dimensional Square Greenhouse

The previous numerical two-dimensional square greenhouse scale model was extended to a three-dimensional cubical cavity. The results were firstly compared to experimental results for a 200mm cube found in the literature by Küreckci and Özcan [15], who investigated the natural convection of a cubical cavity both experimentally and numerically. This is again done to increase confidence in the current CFD models developed for the greenhouse. The cubical enclosure numerically modelled has dimensions of 200mm x 200mm x 200mm to be able to compare to Kürekci et al [15]. One vertical wall of the cavity was specified a constant temperature of 69°C, while the opposite cold wall was kept at a constant temperature of 41°C. The remainder of the cube walls were adiabatic. The details of the experimental setup to which the current model can be compared can be found in [15]. The gravitational vector is in the negative y-direction in the CFD model. The CFD model was run in the laminar regime to be able to compare to previously published results. To monitor numerical CFD accuracy, a mesh sensitivity analysis was once again conducted. Variables such as temperature, velocity and surface average Nusselt number were monitored. As mentioned by Dol et al [16], three-dimensional high-Reynold number (turbulent) flow is rather complex, and requires a fine mesh in the regions adjacent to the solid walls, therefore 20 prism layers were once again selected, with a combined thickness of 0.02m. A base size of 0.003m was chosen as the temperature no longer varied with a decreasing mesh size. The numerical results obtained for the current 3D square scale model are compared to results obtained in the literature [17]. A difference of 5.04% was found between the numerical obtained Surface Averaged Nusselt number and the Nusselt number found by Kürekci [17]. Therefore additional confidence has again been established in the current three-dimensional CFD model of a cubical enclosure. A more detailed comparison can be found in [18]. To enable the comparison of the two-and three-dimensional cavities, a three-dimensional model with dimensions 0.75m x 0.75m x 0.75m was created in StarCCM+ for the current research. This was done in order to ascertain the influence of a third dimension on temperature and velocity distributions. The same approach as described previously was used to model the original 0.75m greenhouse with zero degree roof angle as a three-dimensional cube, and the results can then be compared to the two-dimensional case. The top and bottom walls were specified as 15.1°C and 55.1°C ($Ra = 1.35 \times 10^9$) respectively. The sidewalls were all specified as adiabatic. The base size, number of prism layer and prism layer thickness were all kept the same as in the two-dimensional case.

The simulated CFD temperature contour plots for the two cases are compared in Figure 2. For the three-dimensional case, the contour plot was taken in the $z/H = 0.5$ plane. The temperature contours for the two-dimensional case tends to be more circular, whereas the contours for the three-dimensional case tend to be slightly more of square shape. This is also visible in the velocity vector plots (Figure 3). The vector plot for the two-dimensional case also shows two secondary convective cells in the top left and bottom right corners. This is not present in the three-dimensional case. The temperature difference through the boundary layer to the uniform core region for the three-dimensional case is not as steep as for the two-dimensional case, which is visible in the temperature distribution plot (Figure 4). The centre of the cavity is at the same temperature for both cases. As far as velocity distribution in the centre of the cavity is concerned (Figure 5), quite a significant difference is noticed between the two-and three-dimensional case. Both cases exhibit the same trend of reaching a maximum adjacent to the walls, and decreasing towards the centre. The maximum velocity reached in the two-dimensional case is 0.33 m/s whereas a velocity of 0.22 m/s is reached in the three-dimensional case.

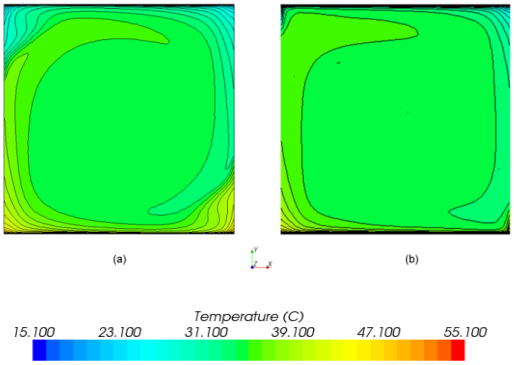

Figure 2: Temperature contour plot comparison for (a) Two-dimensional case (b) Three-dimensional case (z/H=0.5)

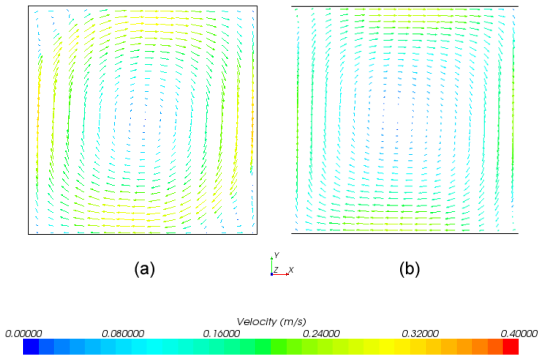

Figure 3: Vector plot comparison for (a) Two-dimensional case (b) Three-dimensional case (z/H=0.5)

.

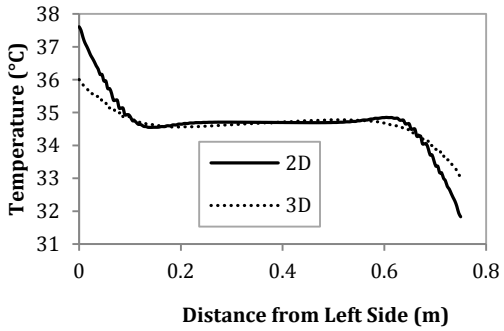

Figure 4: Comparison of temperature distribution in the centre of the cavity

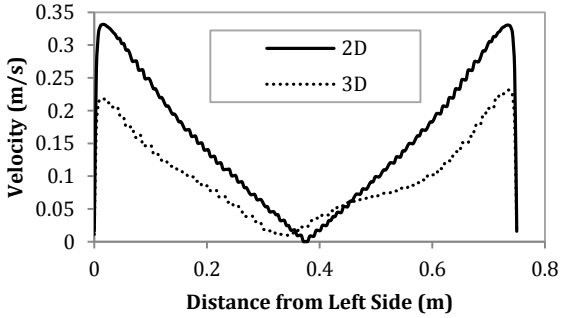

Figure 5: Comparison of velocity distribution in the centre of the cavity

The Nusselt number distribution calculated as indicated previously from CFD results is shown in the 3D surface plot in Figure 6. The maximum Nusselt number is visible towards the front right corner. The average Nusselt number was calculated to be 77.3. The Nusselt number for the two-dimensional case was 78.7, which amounts to a difference of 1.8%.

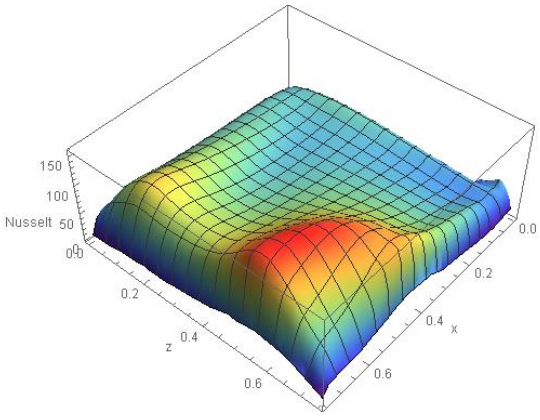

Figure 6: Nusselt Number distribution on the floor of the cube

Three-dimensional Modified Greenhouse

Two types of three-dimensional greenhouses have been numerically investigated. The first greenhouse had a roof angle of 30 degrees, whereas the second greenhouse had a roof angle of 45 degrees. The average Nusselt number on the floor of the cavity was calculated as shown in equation 6, and compared to the average Nusselt number for each of the two-dimensional cases. The results are plotted in Figure 7 and Figure 8 respectively. From Figure 7 it can be seen that there is not as significant difference in the calculated average

Nusselt Number on the floor of the cavity for the two and three-dimensional cases (for a greenhouse with a 30 degree roof angle). The difference increases with increasing Rayleigh number. For the highest Rayleigh number (1.9 x 109) the difference average Nusselt number is 2.35%. If the roof angle is increased to 45 degrees, the difference between the two-dimensional and three-dimensional average Nusselt numbers is quite noticeable. For the lowest Rayleigh number (2.22×10^8) the difference is 18.6% and for the largest Rayleigh number the difference increases to 51%.

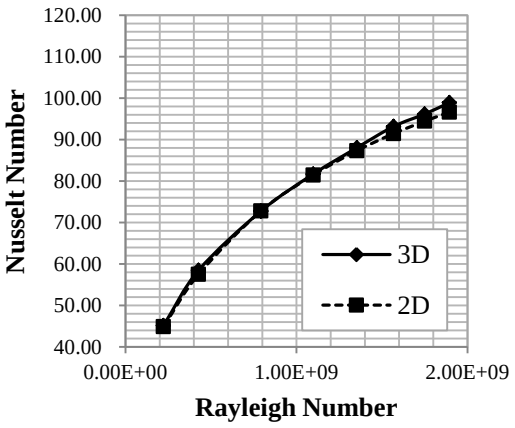

Figure 7: Average Nusselt Number on the Hot Wall for 2D and 3D for a 30 Degree Roof Greenhouse

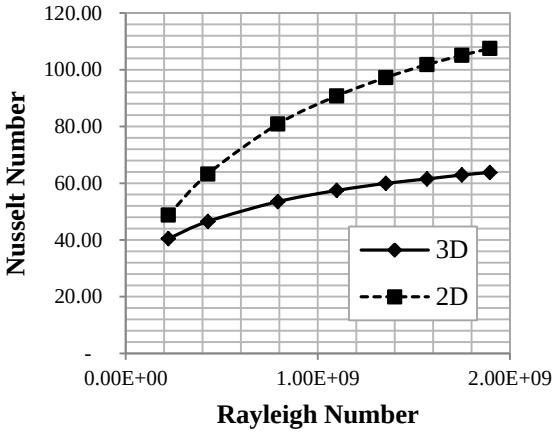

Figure 8: Average Nusselt Number on the Hot Wall for 2D and 3D for a 45 Degree Roof Greenhouse

The Nusselt-Rayleigh relationships that best fit the above simulated curves for the three-dimensional models have been deduced from the previous plots and are tabulated in Table 1.

Table 1: Nusselt-Rayleigh Relationships

Roof Angle	Nusselt-Rayleigh Relationship
30°	$Nu = 0.047Ra^{0.3584}$
45°	$Nu = 0.6646Ra^{0.2139}$

Three-dimensional Models with a 30 Degree Roof Angle

To continue the investigation of the heat transfer characteristics in a three-dimensional greenhouse, the case of a greenhouse with a 30 degree roof angle will be discussed in more detail here. It was decided to focus on only three Rayleigh numbers: 4.27×10^8, 1.35×10^9 and 1.9×10^9. These three Rayleigh numbers correspond to a temperature difference between the roof and the floor of the greenhouse of 10°C, 40°C and 70°C respectively. The isotherms in three different planes (front, middle and back) are shown in Figure 9 for the three chosen Rayleigh numbers. The temperatures for the smallest Rayleigh number (Figure 9a) are relatively low, with higher temperatures close to the floor. The temperatures are also homogeneously distributed throughout the height and width of the cavity. If the Rayleigh number is increased to 1.35×10^9 (Figure 9b) the temperatures are slightly higher compared to the lowest Rayleigh number, and also more non-uniform. The isotherms become distorted, with more densely spaced temperature contours at the bottom adjacent to the heated floor in the front of the cavity. At the back of the cavity the temperature is slightly higher compared to the rest of the cavity, indicating lower heat transfer. The temperature contours for the highest Rayleigh number, 1.9×10^9 indicates a high temperature at the bottom in front of the greenhouse, with a larger uniform temperature region in the centre of the greenhouse toward the back of the greenhouse. Figure 10 shows the temperature distribution at mid-height for the three locations in the greenhouse for the lowest Rayleigh number. This figure indicates that the temperature distribution varies quite significantly from the front to the back of the cavity. The center of the greenhouse has a homogenous temperature distribution, whereas the front of the greenhouse reaches it maximum temperature at approximately 0.2m from the left wall. The temperatures reach a minimum at the walls in the font of the greenhouse. At the back of the greenhouse temperatures are slightly higher, especially toward the left wall.

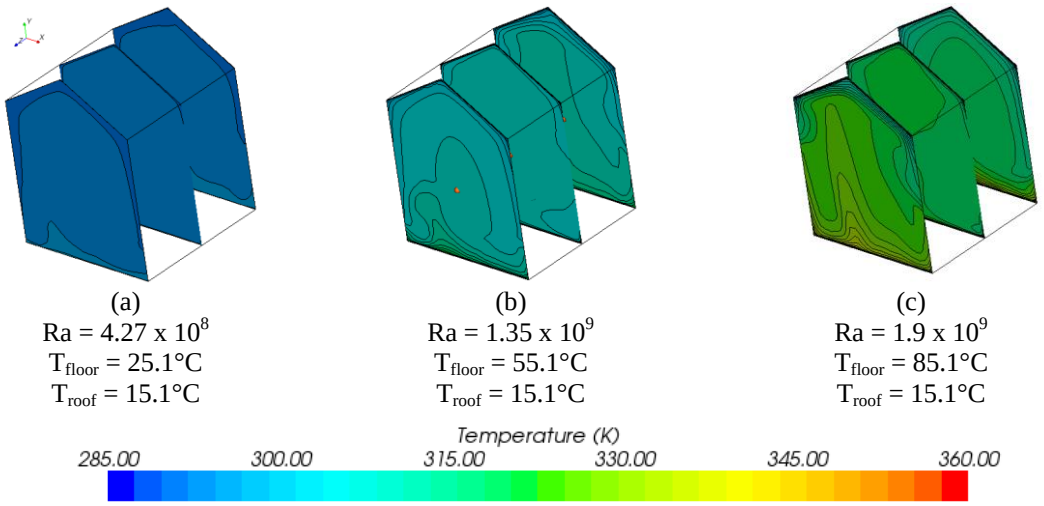

Figure 9: Temperature Distribution in three planes (30 Degree Roof Angle)

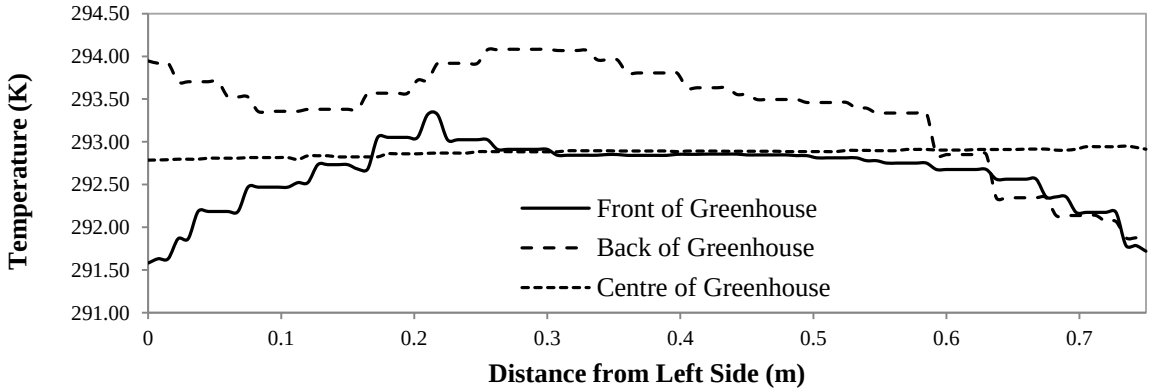

Figure 10: Temperature distribution in three planes (front, middle, back) for Ra = 4.27 x 10^8

The temperature distribution at mid-height for Ra = 1.35 x 10^9 are shown in Figure 11. The temperature in the front of the cavity at mid-height is characterized by a parabolic type distribution. The maximum temperature reached is similar to the temperature in the centre of the greenhouse (306K). The center of the greenhouse has a uniform temperature distribution at mid-height, whereas the temperature increases toward the back of the greenhouse with a maximum temperature of 311K. The temperature is lower at the back of the greenhouse adjacent to the right wall. This graph also shows the temperature plots are horizontal at the left and right wall, indicating that these walls are adiabatic.

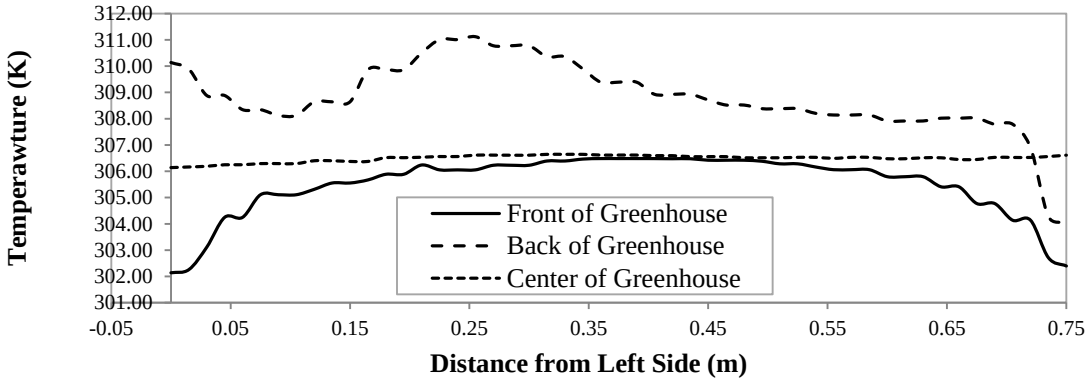

Figure 11: Temperature distribution in three planes (front, middle, back) for Ra = 1.35 x 10^9

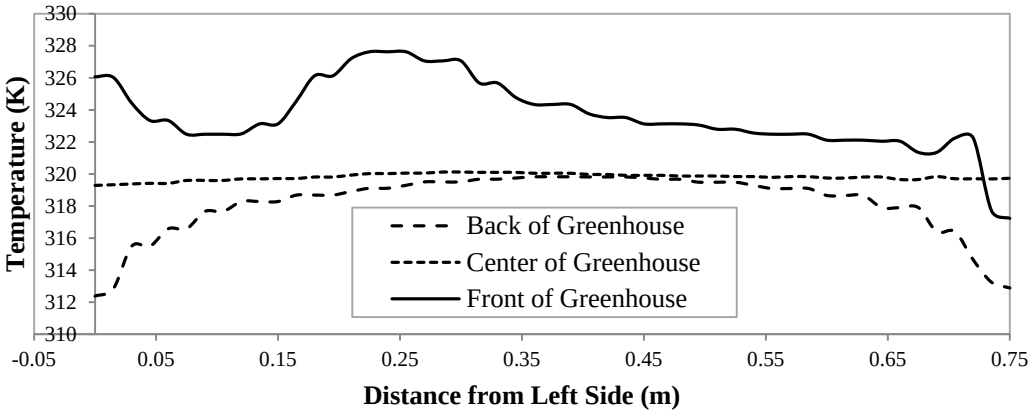

Figure 12: Temperature distribution in three planes (front, middle, back) for Ra = 1.9 x 10^9

The scenario changes for the highest Rayleigh number as shown in Figure 12. In this case the front of the greenhouse exhibits the highest temperature distribution, the center is once again homogeneous, and the back of the greenhouse shows a parabolic type temperature distribution. The maximum temperature reached in the back of the greenhouse is similar to the temperature reached in the centre of the greenhouse. The Nusselt number distribution for the three cases is shown in Figure 13. From this figure it can be seen that there are two areas of maximum heat transfer for each case. For the two lower Rayleigh numbers the two areas of maximum heat transfer – adjacent to the left wall and in the bottom right corner. For the maximum Rayleigh number the areas of maximum heat transfer moves to the two top corners, which is actually located at the back of the greenhouse. The location of the maximum heat transfer is due to convective recirculation (not shown here) impinging at these locations on the floor. These plots correlate with the temperature distributions given in the previous figures. The low heat transfer rate in the front of the greenhouse for the highest Rayleigh number is responsible for the higher temperature as seen in Figure 12.

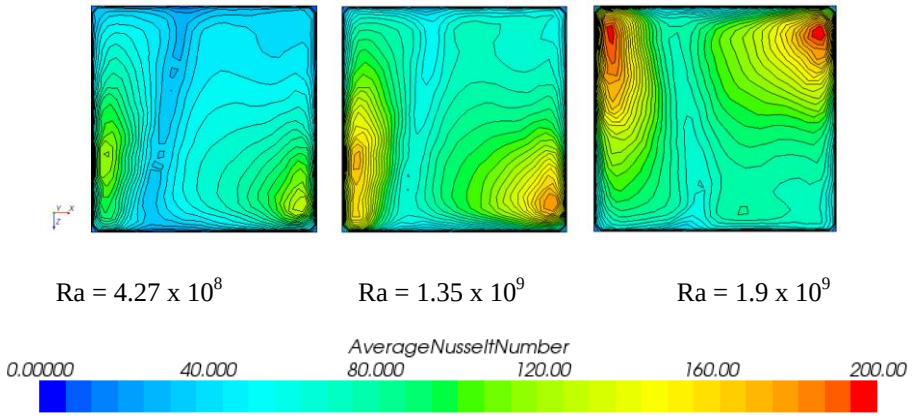

Figure 13: Nusselt Number Distribution on hot floor (30 Degree Roof Angle)

CONCLUSION

In this paper a numerical investigation was conducted to investigate the heat transfer in two and three-dimensional cavities corresponding to a model of a single span greenhouse. Initially the CFD models were verified using results found in the literature for a square and cubical cavity. The CFD results correlated well with the experimental results. The three-dimensional model was modified to include a roof angle of 30 degrees and 45 degrees respectively and compared to similar two-dimensional models. When the average Nusselt numbers on the floor (hot wall) were compared, it was found that the difference was minimal for the 30 degree roof angle, but was quite significant in the case of a 45 degree roof angle. Nusselt-Rayleigh relationships were also deduced for the 30 and 45 degree roof angle cavities. The heat transfer of the 30 degree roof angle cavity was further investigated in more detail, and it was shown that the maximum heat transfer was not always found in the same location on the floor of the three dimensional cavity. The

temperature distributions for various plane sections through the cavity also indicated that temperatures varied throughout the greenhouse. These temperature variations can become important once crops are present, as non-uniform temperature distributions in a greenhouse can lead to non-uniform crop yield. The differences between the 3D and 2D heat transfer characteristics for the 30 degree and 45 degree greenhouse is a topic to be addressed in future research.

REFERENCES

[1] W. D. Baines and J. S. Turner, "Turbulent Buoyant convection from a source in a confined region," *Journal of Fluid Mechanics,* vol. 37, pp. 51-80, 1969.

[2] M. A. Lamrani, T. Boulard, J. C. Roy and A. Jaffrin, "Airflows and Temperature Patterns induced in a Confined Greenhouse," *Journal of Agricultural Engineering Research,* vol. 78, no. 1, pp. 75-88, 2001.

[3] W. H. Leong, K. G. T. Hollands and A. P. Brunger, "On a physically!realizable benchmark problem in internal natural convection," *International Journal of Heat and Mass Transfer,* vol. 41, pp. pp 3817 - 3828, 1998.

[4] M. A. Mamun, W. H. Leong, K. G. Hollands and D. A. Johnson, "Cubiical-cavity natural-convection benchmark experiments: an extension," *International Journal of Heat and Mass Transfer,* vol. 46, pp. 3655-3660, 2003.

[5] A. Bairi, "Nusselt–Rayleigh correlations for design of industrial elements: Experimental and numerical investigation of natural convection in tilted square air filled enclosures," *Energy Conversion and Management,* vol. 49, pp. 771 - 782, 2008.

[6] Z. Altec and N. Ugurlubilek, "Assessment of turbulence models in natural convection from two-and three-dimensional rectangular enclosures," *International Journal of Thermal Sciences,* vol. 107, pp. 237-246, 2016.

[7] I. H. Shames, Mechanics of Fluids, New York: McGraw-Hill, 2003.

[8] A. W. Date, Introduction to Computational Fluid Dynamics, New York: Cambridge University Press, 2005.

[9] H. K. Versteeg and W. Malalasekera, An introduction to Computational Fluid Dynamics, The Finite Volume Method,2nd Ed, England: Pearson Prentice Hall, 2007.

[10] CD-Adapco, "StarCCM+ User Guide," CD-Adapco, 2016.

[11] S. V. Patankar, Numerical Fluid Flow and Heat Transfer, New York: Hemisphere, 1980.

[12] M. Aounallah, Y. Addad and S. Benhamadouche, "Numerical investigation of turbulent natural convection in an inclined square cavity with a hot wavy wall," *International Journal of Heat and Mass Transfer,* vol. 50, pp. pp 1683-1693, 2007.

[13] R. A. Henkes, F. F. van der Vlugt and C. J. Hogendoorn, "Natural Convection flow in a square cavity calculated with low-Reynolds-number turbulence models," *International Journal of Heat and Mass Transfer,* vol. 2, pp. 377-388, 1991.

[14] S. Kruger and P. L, "Analysis of Natural Convection in a Mono-Span Greenhouse," in *South African Conference on Applied Mechanics*, Johannesburg, 2012.

[15] N. A. Kurekci and O. Ozcan, "An Experimental and Numerical Study of Laminar Natural Convection in a Differentially-heated Cubical Enxlosure," *Journal of Thermal Science and Technology,* vol. 32, no. 1, pp. 1-8, 2012.

[16] H. S. Dol and K. Hanjalic, "Computational study of turbulent natural convection in a side-heated near-cubic enclosure at a high Rayleigh number," *International Journal of Heat and Mass Transfer,* vol. 44, pp. 2323-2344, 2001.

[17] N. A. Kurecki and O. Ozcan, "An experimental and Numerical Study of Laminar Natural Convection in a differentially-heated Cubical Enclosure," *Journal of Therrmal Science and Technology,* vol. 32, no. 1, pp. 1-8, 2012.

[18] S. Kruger, A NUMERICAL EVALUATION OF MULTI-DIMENSIONAL HEAT TRANSFER EFFECTS IN GREENHOUSES, Johannesburg: University of Johannesburg, 2016.

[19] CD-Adapco, "StarCCM+ User Guide," CD-Adapco, 2012.